PHYSOR 2004 -The Physics of Fuel Cycles and Advanced Nuclear Systems: Global Developments
Chicago, Illinois, April 25-29, 2004, on CD-ROM, American Nuclear Society, Lagrange Park, IL. (2004)

JOYO MK-III Performance Test at Low Power and Its Analysis

Gou Chiba*, Kenji Yokoyama, Shigetaka Maeda and Takashi Sekine

Experimental Reactor Division, Irradiation Center, O-arai Engineering Center
Japan Nuclear Cycle Development Institute
4002 Narita, O-arai, Ibaraki 311-1393 JAPAN

Performance test at low power has been carried out in the experimental fast reactor JOYO for the upgraded MK-III core. In the test, several neutronics characteristics, such as the control rod worth, the control rod shadowing effect, the excess reactivity and the isothermal temperature coefficient have been measured. For the analysis, a deterministic standard calculation method developed by Japan Nuclear Cycle Development Institute was used. Calculated values agreed well with the experimental ones within 0.55%Δk/kk' in the excess reactivity, 4% in the control rod worth and 3% in the isothermal temperature coefficient.

KEYWORDS: fast reactor, JOYO, MK-III, control rod worth, excess reactivity, isothermal temperature coefficient, JENDL-3.2

1. Introduction

JOYO is a Japanese experimental fast reactor whose missions include improvements in fast reactor safety and operation, and especially irradiation testing of advanced fuels and materials. JOYO was recently upgraded to the MK-III design, the second major upgrade since it began operation in 1977. The four main components of the MK-III upgrade are 1) increase in fast neutron flux and enlargement of irradiation space, 2) improved irradiation test subassemblies, 3) modified heat transfer system for the 40% increase in power, and 4) improved plant availability. The first component is the one of primary interests here because it drove most of the changes in the core design including the core volume, fuel enrichment, the control rod layout and the radial reflection configuration. These subassembly loading changes are described in Section 2.

MK-III performance test began in July 2003 to fully characterize the upgraded core and heat transfer system. Results of the test conducted at low power, which focus on the neutronics characteristics, and its analysis by a deterministic standard calculation method developed by Japan Nuclear Cycle Development Institute (JNC) are presented here. A detail of the test is described in Section 3. Comparison between the experimental values and the calculated ones is shown in Section 4.

2. Description of JOYO MK-III Core

The core configurations and main parameters of the MK-II and MK-III cores are shown in Fig. 1 and Table 1. The fuel region is divided into two radial enrichment zones in the MK-III core to flatten the neutron flux distribution.

In the initial MK-III core loading, 75 driver fuel subassemblies were loaded and the central fuel subassembly was replaced by the material irradiation test subassembly with no fissile to offset the excess

* Corresponding author, Tel. +81-29-267-4141, Fax. +81-29-267-1676, E-mail: go_chiba@oec.jnc.go.jp

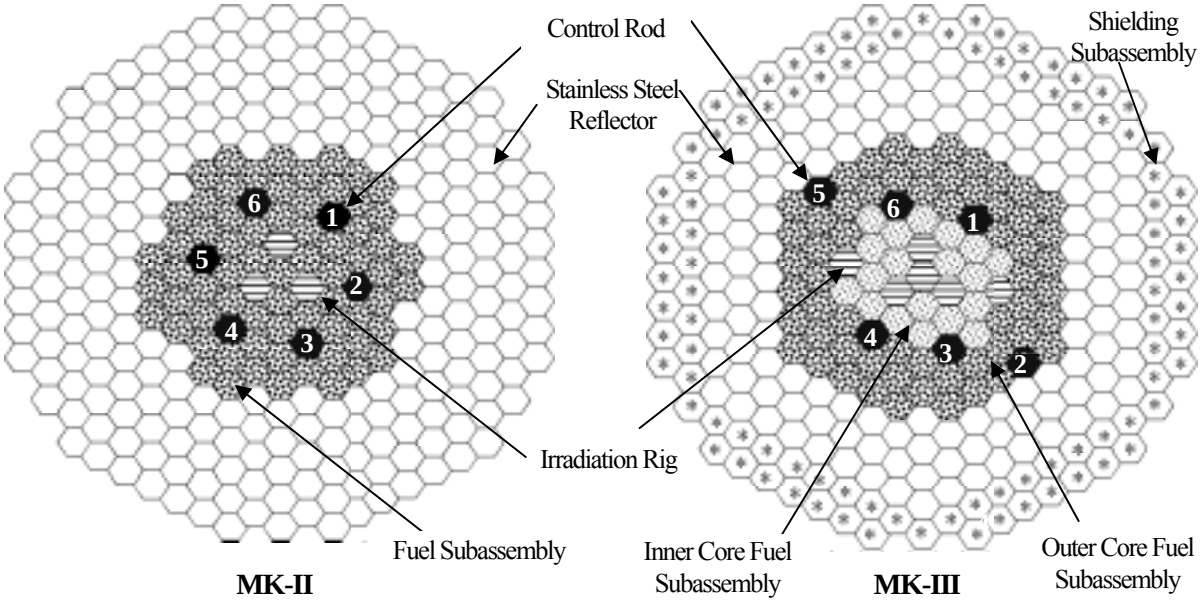

Fig.1 Comparison of JOYO MK-II and MK-III cores used in the core design

reactivity increased by 55 fresh fuel subassemblies. Twenty of the outer core fuel subassemblies had already been loaded and irradiated in the transition core. The change of atomic number density during burn-up in the transition core was calculated by the JOYO core management code system. This code system is based on the diffusion theory for the neutronic calculation and the matrix exponential method for the burn-up calculation.

Two of six control rods (CRs) of which number is shown in Fig. 1, CR No.2 and No.5, were shifted from the third row to the fifth row to provide high-fast-flux loading positions for instrumented-type irradiation subassemblies.

Another change made to enlarge higher neutron flux irradiation field was to increase the maximum number of driver fuel subassemblies from 67 to 85. The equivalent diameter of the initial MK-III core is approximately 80 cm. The maximum number of irradiation test

Table 1 Main core parameters of JOYO MK-II and MK-III cores

Specification			MK-III	MK-II
Reactor Thermal Power		(MWt)	140	100
Max. Number of Driver Fuel Subassemblies*			85	67
Equivalent Core Diameter		(cm)	80	73
Core Height		(cm)	50	55
^{235}U Enrichment		(wt%)	18	18
Fissile Pu Content: (^{239}Pu+^{241}Pu)/(Pu+U)		(wt%)	16/21**	20
Max. Linear Heat Rate of Fuel Pin		(W/cm)	420	400
Max. Burn-up of Fuel(Pin Average)		(GWd/t)	90	75
Max. Fast Neutron Flux (E>0.1 MeV)		(n/cm^2·s)	4.0x10^{15}	3.2x10^{15}
Number of Control Rods	In the Third Row		4	6
	In the Fifth Row		2	0
Reflector/Shielding			SUS/B_4C	SUS/SUS
Primary Coolant Temperature (Inlet/Outlet)		(℃)	350/500	370/500
Operation Period		(day/cycle)	60	70
Number of Cycle		(cycle/year)	5	4

*Including Number of Irradiation Test Fuel Subassemblies

**Inner Core / Outer Core

subassemblies increased from 9 to 21. The core height was decreased from 55 cm to 50 cm to obtain a higher neutron flux with smaller axial power peaking. With these core modifications, the maximum fast neutron flux (E > 0.1 MeV) increased from 3.2×10^{15} n/cm^2·s to 4.0×10^{15} n/cm^2·s and the reactor thermal power increased from 100 MWt to 140 MWt.

It can be seen in Fig. 1 that the outer two rows of radial stainless steel reflectors were replaced by shielding subassemblies, which contain 45 % enriched boron carbide. This reduces the total neutron flux at the in-vessel spent fuel storage rack to about 30 % of the MK-II core value, after accounting for the 40 % reactor power increase. This will lower the fission rate in the stored spent fuel subassembly, making a simple spent fuel cooling system adequate, even with the increased reactor power.

3. Measurement Method Employed in MK-III Performance Test at Low Power

3.1 Control Rod Worth

All the six control rods have the same poison-type design. The poison section contains B_4C enriched to 90% in ^{10}B. The poison section is 650 mm long, which is also the axial distance where the rod can move. The rod position readout at the fully down position is 0 mm and the bottom boundary of the B_4C is at the core axial mid-plane when the rod is half withdrawn (325 mm position).

All the CRs were calibrated by a period-like method. At each calibration step, the core was kept critical before the calibrated rod was withdrawn and positive reactivity was added by the rod withdrawal. It was compensated by an insertion of the other rods. When CR in the third row was calibrated, about 50 steps were necessary. Inserted reactivity was determined by the inverse kinetic algorithm.

CR insertion pattern was changed during the measurement. In order to simplify the comparison of measured CR worth and calculated one, the measured worth at each calibration step was "adjusted" to the value where the other rods not being calibrated are assumed to be fully withdrawn.

The adjustment was done by multiplying an adjustment factor to measured worth at each step. The adjustment factor was obtained from the ratio of calculated worth between the assumed CR insertion pattern and that in the actual measurement. The calculations were carried out by a diffusion theory code with 7-group cross sections. It will be shown in the analysis of a CR shadowing effect experiment that the coarse calculation is accurate enough to evaluate the adjustment factors.

3.2 Control Rod Shadowing Effect

The CR shadowing effect is a change of the CR worth in the different insertion patterns of the other CRs. The shadowing effect is defined as a ratio of the CR worth in the different insertion patterns.

When a calibrated CR was withdrawn in the period-like method, the other CRs must be inserted for compensation of reactivity because the core must be kept critical. The change of the CR position for the reactivity compensation causes another shadowing effect. However, we could make the other shadowing effect negligible by using CRs in the fifth row for the compensation. In the test, measurements of shadowing effect of CR No.1 and No.5 were carried out.

3.3 Excess Reactivity

Because of significant changes in the core subassembly loading, approach to criticality was carried out cautiously. At each rod withdrawal step, counts of source-range monitors were

measured. Inverse count rate was plotted versus calculated reactivity insertion to realize secure approach to criticality.

The excess reactivity is defined when all the CRs are fully withdrawn. To determine the reactivity, the integrated control rod worth are required so that all the CRs are inserted to the same depth. The CR worth measured by the period-like method were adjusted using the diffusion calculation with the same procedure described in the Section 3.1.

3.4 Isothermal Temperature Coefficient

To begin the measurement, a uniform temperature of approximately 250 ^{o}C was established throughout the primary system (isothermal), and the excess reactivity was determined. Next the reactor power was increased in 20-degree steps, measuring excess reactivity at each step, until the primary system reached approximately 350 ^{o}C. Then the reactor temperature was brought back to 250 ^{o}C for isothermal temperature coefficient measurement with the temperature decreasing in 20-degree steps. The temperature was decreased by cooling the sodium using the natural air circulation in the dump heat exchangers. The ascending and descending measurements were repeated, providing four measurements of the coefficients.

4. Analysis and Comparison with the Measurement

4.1 Subassembly Calculation

As the nuclear data, a multi-group library based on JENDL-3.2 [1], which is composed of the infinite dilution cross sections, the scattering matrices and the self-shielding factors, was used. Neutron energy from 10^{-5} eV to 10 MeV is divided into 70 groups in which a lethargy width of each group is 0.25 except for the 70th group (10^{-5} - 0.3 eV).

The fuel subassemblies and control rods were modeled in a two-dimensional pin-by-pin geometry. The other subassemblies, such as the irradiation and shielding subassemblies, etc., were treated homogeneously. All the subassemblies except for the control rods were assumed to be infinite lattice. Critical buckling was introduced to fuel subassembly calculations.

In heterogeneous subassembly calculations, homogeneous-equivalent background cross section was determined by a method proposed by Tone (Tone's method) [2]. The sub-group method is popular and commonly used for an evaluation of the self-shielding effect in heterogeneous cell, but it was shown that a difference between the two methods are negligible in power reactor subassembly calculations [3]. Tone’s method is based on the narrow-resonance approximation. The approximation was validated by a comparison with the ultra-fine energy group calculations below 41 keV. Homogenization was carried out using a flux distribution obtained by the collision probability method. Benoist's anisotropic diffusion coefficients [4] were also calculated.

Control rod calculations were performed in a model where CR is surrounded by six homogenized fuel subassemblies (super-cell model). The reaction rate ratio preservation method [5] was adopted for the homogenization. Reactivity before and after the homogenization are almost same owing to the adoption of the reaction rate ratio preservation method.

Group collapsing of effective cross sections was carried out by using neutron spectra obtained by the diffusion calculation in the hexagonal-Z core model as a weight function.

4.2 Effective Delayed Neutron Fraction

The effective delayed neutron fraction β_{eff} was calculated by a diffusion theory code with 18-group cross sections. Nuclear data used here were Tuttle’s one for the fission yield,

Saphier's one for the delayed fission spectrum and Keepin's one for the delayed neutron family fraction and the decay constant. Calculated β_{eff} was 4.238×10^{-3}. Uncertainty of β_{eff} in the MK-I core was evaluated to be about 3% using the sensitivity coefficients for β_{eff} and uncertainty of the fission yield which was evaluated by Tuttle [6]. Therefore, we assume the uncertainty of β_{eff} in the MK-III core is 3% considering the similarity of the core size and fissile contents between the MK-I and MK-III cores. In the present study, the uncertainty was included in the experimental uncertainty. Therefore, the uncertainty of β_{eff} becomes dominant in the experimental uncertainty of the several neutronics characteristics, such as the CR worth and the excess reactivity.

4.3 Control Rod Worth

The CR worth was calculated using two k_{eff}s obtained by the transport calculations with 7-group cross sections in the XYZ geometry model. It was confirmed that the modeling effect of XYZ core model and the energy group collapsing effect are negligible. S_8-P_0 with the transport approximation was used. The transport cross section was defined as $\Sigma_{tr} = 1/(3D)$ where D means the Benoist's isotropic diffusion coefficient. These conditions for transport calculations were used commonly in the present study. A convergence condition of k_{eff} was set to be 10^{-6}.

Full- and half-traveled CR worth were calculated. Experimental (E-) values with their uncertainty and C/E values are shown in Table 2 and Fig. 2. Calculated (C-) values agree with E-values within 4%. Discrepancies of C/E values between CR No.5 and No.6 are about 3% for the full-traveled worth and 5% for the half-traveled worth. That is larger than the experimental error except for β_{eff} –related uncertainty which is about 1.5 %. The cause is under investigation.

Table 2 Experimental values with their uncertainty of control rod worth

		No. 1	No. 2	No. 3	No. 4	No. 5	No. 6
Full-traveled	Exp. (%Δk/kk')	1.996	0.762	1.975	1.994	0.743	2.001
	Error (%)	3.4	3.5	3.4	3.4	3.5	3.4
	[Error in Cent (%)*]	1.5	1.7	1.5	1.4	1.8	1.4
Half-traveled	Exp. (%Δk/kk')	1.132	0.422	1.115	1.133	0.415	1.137
	Error (%)	3.4	3.5	3.4	3.4	3.5	3.4
	[Error in Cent (%)]	1.5	1.8	1.5	1.5	1.8	1.5

* Experimental error except for β_{eff} -related uncertainty

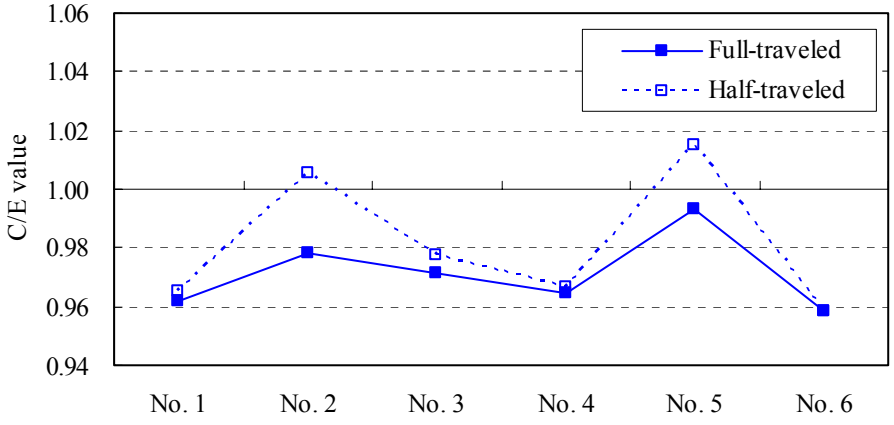

Fig. 2 C/E values of control rod worth

4.4 Control Rod Shadowing Effect

The CR shadowing effect was measured at four cases. For example, in Fig. 3, CR No.1 is assumed as a measured rod and CR No.4 is a shadowing one. The shadowing effect is defined as a ratio of CR No.1 worth with CR No.4 position of 325 mm to that with CR No.4 at 650 mm. Flux tilt caused by CR No.4 insertion from 650 mm to 325 mm increases neutron flux in CR No.1 position. That results in an increase of CR No.1 worth. On the other hand, flux tilt caused by CR No.6 insertion, which is the most adjacent one to CR No.1, results in a decrease of CR No.1 worth.

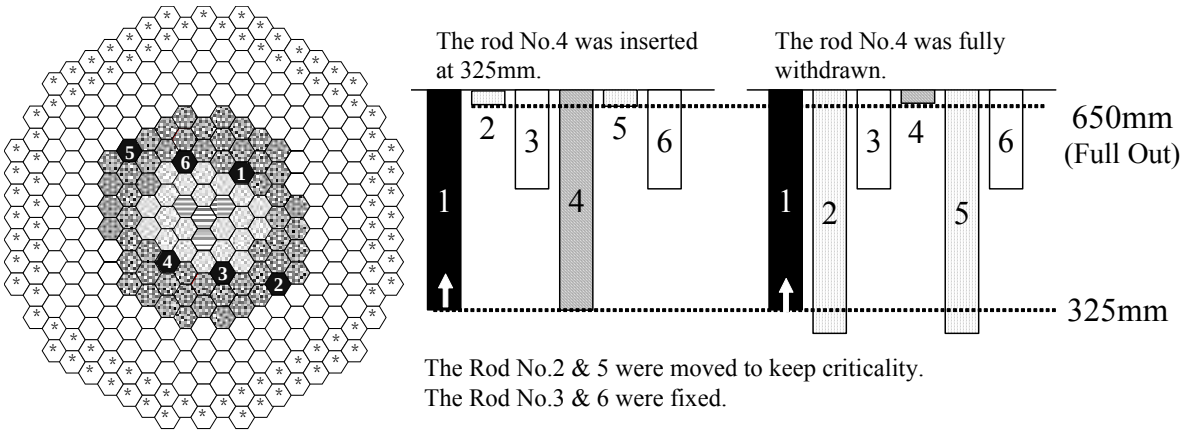

Fig. 3 Control rod pattern of shadowing effect measurement

The shadowing effect was evaluated by both the diffusion and transport calculations with 7-group cross sections. The hexagonal-Z and XYZ core models were used for the diffusion and transport calculations, respectively. The condition of the diffusion calculation was the same as the one used for the adjustment of measured reactivity in the CR calibration. Results are shown in Table 3. The transport calculation results agree with E-values better than those by the diffusion calculation, but the difference between the diffusion and transport calculations is small. In case A, observed disagreement between C- and E- values is larger than the experimental error. These results are reflected to evaluate uncertainty of CR worth.

Table 3 Analysis of control rod shadowing effect

Case	Measured Rod No.	Shadow Rod No.	Rod Worth Change		
			Experimental	Diffusion calculation	Transport calculation
A	1 (325-380 mm*)	4 (325mm/650mm**)(2,5***)	5.7% (±1.2%)	3.2%	3.0%
B	1 (325-430 mm)	6 (325mm/650mm)(2,5)	-7.4% (±1.1%)	-6.2%	-7.2%
C	5 (325-650 mm)	3 (200mm/450mm)(1,4)	6.4% (±0.7%)	5.4%	5.7%
D	5 (325-650 mm)	6 (200mm/450mm)(1,4)	-13.6% (±0.8%)	-11.9%	-14.2%

* Calibrated range

** Positions of shadow rod

*** Compensation rod for shadow rod movement

4.5 Excess Reactivity

Base calculation of the excess reactivity was carried out by a diffusion theory code with 70-group cross sections in the triangle-Z core model. The transport and mesh effect and the core expansion effect were corrected. In addition to the deterministic calculation, the Monte Carlo code MVP [7] was also applied. Results are shown in Table 4. Differences between C- and E- values are 0.55 %Δk/kk' in the deterministic calculation and 0.08 %Δk/kk' in the MVP calculation. The differences are not significant in comparison with the results of the MK-I and MK-II core analyses [8].

In the large-size fast reactor analyses, the differences between deterministic and MVP calculations are within 0.1 %Δk/kk' [9]. In comparison with the large-size fast reactor, the difference of the MK-III core is large. It is considered that the difference was caused by the transport approximation for the neutron anisotropic scattering and the infinite lattice calculations for the reflector subassemblies in the deterministic calculation method.

Table 4 C-E values of excess reactivity

		Deterministic	MVP
Effective multiplication factor	Base calculation	1.0131	1.0346 (±0.0003)
	Transport&mesh effect	+0.0165	
	Core expansion effect	-0.0046	←
	After correction	1.0250	1.0300
Excess reactivity (%Δk/kk')	C-value	2.44	2.91
	E-value	2.99 (±0.09)	←
C-E (%Δk/kk')		-0.55	-0.08

4.6 Isothermal Temperature Coefficient

The isothermal temperature coefficient is composed of the Doppler and core expansion reactivity. These were evaluated separately, which was validated through a comparison with a result obtained by a no-separate evaluation. The Doppler reactivity was calculated by the exact perturbation theory while the core expansion reactivity was obtained directly by difference of two k_{eff}s. Base calculations were performed by a diffusion theory code with 70-group cross sections in the triangle-Z core model and the transport and mesh effect was corrected.

Results of calculations for both components are shown in Table 5. The core expansion component is dominant and the Doppler is about 15% of the isothermal temperature coefficient. C/E values are shown in Table 6. C-value agrees with E-values within 3%.

Table 5 Results of calculations for Doppler and core expansion reactivity (unit: %Δk/kk'/T)

	Dopplar reactivity	Core expansion reactivity
Base calculation	-0.00066	-0.00352
Transport&mesh effect	+0.00001	+0.00037
After correction	-0.00065	-0.00315

Table 6 C/E values of isothermal temperature coefficient

Measurement Date	Temperature Direction	Experimental Coef. (%Δk/kk'/T)	Calculated Coef. (%Δk/kk'/T)	C/E
2003/8/26	ascending	-0.00369	-0.0038	1.03
2003/8/28	ascending	-0.00375		1.01
2003/8/27	descending	-0.00386		0.98
2003/8/29	descending	-0.00385		0.99

5. Conclusion

The core performance of the upgraded JOYO MK-III was successfully evaluated by a series of reactor physics tests. The measurements provided benchmark data for nuclear data library and testing reactor calculations.

The deterministic standard calculation method developed by JNC was used for the analysis. Calculated values agreed well with the experimental ones within 0.55 %Δk /kk' in the excess reactivity, 4% in the control rod worth and 3% in the isothermal temperature coefficient.

As a result, it was found that further investigation is required in the analysis. In the control rod worth, a discrepancy of C/E values between CRs in the third and the fifth rows are observed, especially for the half-traveled worth. In the excess reactivity, a difference between the results obtained by the deterministic method and the statistical method was about 0.5%Δk/kk'.

Acknowledgements

We would like to appreciate Dr. R. W. Schaefer from Argonne National Laboratory for his valuable comments and discussions about the performance test results. Many persons at JOYO are responsible for the design, execution and analysis of the MK-III performance tests. K. Numata of NESI Inc. performed the isothermal temperature coefficient calculation.

References

1) T. Nakagawa, et al, "Japanese Evaluated Nuclear Data Library Version 3 Revision-2: JENDL-3.2," J. Nucl. Sci. Technol. 32[12], pp.1259-1271 (1995).
2) T. Tone, "A Numerical Study of Heterogeneity Effects in Fast Reactor Critical Assemblies," J. Nucl. Sci. Technol. 12[8], pp. 467-481 (1975).
3) G. Chiba, "A Combined Method to Evaluate the Resonance Self Shielding Effect in Power Fast Reactor Fuel Assembly Calculation," J. Nucl. Sci. Technol. 40[7], pp.537-543 (2003).
4) P. Benoist, "Streaming Effects and Collision Probabilities in Lattices," Nucl. Sci. Eng. 34, pp. 285-307 (1968).
5) T. Kitada, et al, "New Control Rod Homogenization Method for Fast Reactors," J. Nucl. Sci. Technol. 31[7], pp. 647-653 (1994).
6) R. J. Tuttle, "Review of Delayed Neutron Yields in Nuclear Fission," Proc. Consultants' Mtg. Delayed Neutron Properties, Vienna, Austria, March 26-30, 1979, INDC-NDS-107/G Special, p.29, International Atomic Energy Agency (1979).
7) T. Mori and M. Nakagawa, "MVP/GMVP: General Purpose Monte Carlo Codes for Neutron and Photon Transport Calculations based on Continuous Energy and Multigroup Methods," JAERI-Data/Code 94-007, Japan Atomic Energy Research Institute, (1994) [in Japanese].
8) K. Yokoyama, et al, "Development of a Standard Database for FBR Core Nuclear Design (XI) Analysis of the Experimental Fast Reactor "JOYO" MK-I Start-up Test and Operation Data," JNC TN9400 2000-036 [in Japanese].
9) M. Ishikawa, "Consistency Evaluation of JUPITER Experiment and Analysis for Large FBR Cores," Proc. of Int. Conf. on the Physics of Reactors (PHYSOR96), Mito, Japan, Vol. 2, P. E-36, (1996).